DOI 10.1002/pmic.200701048 *Proteomics* 2008, *8,* 2104–2114

RESEARCH ARTICLE

Quantitative analysis of *Streptococcus pneumoniae* TIGR4 response to *in vitro* iron restriction by 2-D LC ESI MS/MS

Bindu Nanduri[1, 2], Pratik Shah[3], Mahalingam Ramkumar[4],Edward B. Allen[2, 4], Edwin Swiatlo[5], Shane C. Burgess[1, 2, 6, 7] and Mark L. Lawrence[1, 2]**

[1] College of Veterinary Medicine, Mississippi State University, MS, USA
[2] Institute for Digital Biology, Mississippi State University, MS, USA
[3] Department of Microbiology, University of Mississippi Medical Center, Jackson, MS, USA
[4] Department of Computer Science and Engineering, Mississippi State University, MS, USA
[5] Research Service (151), Veterans Affairs Medical Center, Jackson, MS, USA
[6] Mississippi Agriculture and Forestry Experiment Station, Mississippi State University, MS, USA
[7] Life Sciences and Biotechnology Institute, Mississippi State University, MS, USA

Understanding the growth of bacterial pathogens in a micronutrient restricted host environment can identify potential virulence proteins that help overcome this nutritional barrier to productive infection. In this study, we investigated the pneumococcal protein expression response to iron limitation using an *in vitro* model. We identified *S. pneumoniae* TIGR4 proteins by 2-D LC ESI MS/MS and determined significant changes in protein expression in response to iron restriction using computer-intensive random resampling methods. Differential protein expression was studied in the context of a *S. pneumoniae* TIGR4 protein interaction network using Pathway Studio. Our analysis showed that pneumococcal iron restriction response was marked by increased expression of known virulence factors like PsaA. It involved changes in the expression of stress response, and phase variation and biofilm formation proteins. The net effect of changes in all these biological processes could increase the virulence of *S. pneumoniae* TIGR4 during *in vivo* infection.

Received: November 20, 2007
Revised: January 11, 2008
Accepted: January 22, 2008

Keywords:
Interaction networks / Iron restriction / Monte Carlo / Pathogenesis / Random resampling with replacement

Correspondence: Dr. Bindu Nanduri, College of Veterinary Medicine, Box 6100, Mississippi State University, MS 39762, USA
E-mail: bnanduri@cvm.msstate.edu
Fax: +1-662-325-1031

Abbreviations: DnaK molecular chaperone DnaK; **FDR,** false discovery rate; **GO,** Gene Ontology; **HPr,** phosphocarrier protein HPr; **MudPIT,** multidimensional protein identification technology; **PtsI,** phosphoenolpyruvate-protein phosphotransferase; **PyrG,** CTP synthetase; **RR,** resampling statistics with replacement; **SCX,** strong cation exchange; **UDP,** uridine diphosphate

1 Introduction

Streptococcus pneumoniae is the most common etiologic agent in a number of human diseases including otitis media, sinusitis, bacterial meningitis, sepsis, and pneumonia [1]. Though primarily a commensal in the nasopharynx of up to 60% of healthy children and 30% of healthy adults where it colonizes asymptomatically [2], infection of lungs, blood, and

* Both authors contributed equally to this work.

brain define invasive pneumococcal disease, causing considerable morbidity and mortality worldwide. Productive pneumococcal infection requires adaptation of the pathogen to the host microenvironment. Understanding *S. pneumoniae* mechanisms to overcome physiological stresses during the course of infection will identify potential virulence determinants of pneumococcal disease.

Growth of pathogens under iron restricted conditions is one of the approaches for identifying host specific protein expression [3]. Iron restriction offers intriguing insights into the interplay between host defense and bacterial adaptation to environmental stress. Iron is an essential micronutrient for bacterial growth. Yet, high concentrations of iron are toxic; therefore the human host restricts its availability *in vivo*. The concentration of free iron in human body is 10^{-18} M, which does not support bacterial infection [4]. Thus, iron acquisition, a fundamental physiological function, overlaps with virulence in pathogenic bacteria that overcome this nutritional barrier for productive infection.

In vitro growth of pathogens in iron restricted culture medium mimics the *in vivo* iron restriction that the pathogen has to overcome to establish productive infection [5]. Some bacteria that colonize the upper respiratory tract in human secrete small molecular weight compounds called siderophores that bind iron with high affinity [6]. The host defense to this form of bacterial iron acquisition is the expression of siderocalin that sequesters bacterial encoded siderophores. *S. pneumoniae* iron acquisition is not mediated by siderophores, therefore it utilizes siderocalin mediated host antimicrobial defense to its selective advantage for clearing other pathogenic bacteria that depend on siderophores for survival. Mouse models of nasopharyngeal colonization of *S. pneumoniae* identified 65-fold increase in siderocalin gene expression [7]. Thus studying the effects of iron restriction in the context of pneumococcal disease can unveil important factors necessary for *S. pneumoniae* pathogenesis.

The availability of genome sequences for *S. pneumoniae* led to the identification of genes and proteins that are involved in virulence and pathogenesis [8]. However, genome sequences cannot reveal environmentally controlled virulence factors or factors induced at different stages of infection in the host [9]. To date, there are no reported studies that address the effects of iron restriction at the molecular genomic level. Therefore, the objective of this study is to determine quantitative changes in protein expression of *S. pneumoniae* TIGR4, a clinical isolate, in response to iron restriction using multidimensional protein identification technology (MudPIT).

We also describe analysis of 2-D LC ESI MS/MS proteomics data using computer-intensive Monte Carlo random resampling statistics with replacement (RR) [10–12] for differential quantitative proteomics. We identified significant differences in expression of proteins specific to *in vitro* iron restriction. Proteins differentially expressed in response to iron restriction may represent an important subset of pneumococcal proteins that contribute to virulence and pathogenesis *in vivo*. Systems biology modeling of our proteomics data using a *S. pneumoniae* protein interaction network suggests that the iron restriction response of *S. pneumoniae* TIGR4 involves changes in the expression of known virulence factors. Additional changes included stress response, phase variation, and biofilm formation proteins. All of these biological processes would lead to enhanced virulence in the host.

2 Materials and methods

2.1 Bacterial strains, media, and growth conditions

S. pneumoniae strain TIGR4 [13] was grown in THY medium, Todd-Hewitt broth supplemented with 0.5% yeast extract (Difco Laboratories, Detroit, MI), to obtain cells grown under iron replete conditions. To harvest cells grown under iron restricted conditions, THY medium was cation depleted by adding Chelex-100 (BioRad, Hercules, CA) to a final concentration of 5% for 8 h with continuous agitation. Chelex-100 contains iminodiacetate bound to polystyrene beads and binds polyvalent cations with high affinity. In addition to iron, pneumococci require only calcium, magnesium, and manganese for growth, so these are the cations supplemented after chelation. This method for growing pneumococci in iron-restricted media has been used by many investigators in published studies of iron utilization by pneumococci [14, 15].

The Chelex-100 was removed by filter sterilization, and the medium was supplemented with 100 μM calcium chloride, 2 mM magnesium sulfate, and 1 mM manganese chloride. Cells were harvested from triplicate cultures under iron replete and iron restricted conditions from mid-log phase ($OD_{600\,nm}$ ~0.4–0.6) of growth by centrifugation. The harvested pellets were washed twice in sterile PBS (pH 7.0) and stored at −80°C.

2.2 Protein isolation

Protein isolations and subsequent proteomic analysis was carried out with triplicate samples of *S. pneumoniae* TIGR4 grown under iron replete and iron restricted growth conditions. *S. pneumoniae* pellets were lysed in 7 M urea, 2 M thiourea, 60 mM DTT, 4% CHAPSO, and 8 mM PMSF by sonication in four 5 s pulses on ice (Branson Sonifier 250, Branson Ultrasonics) and then pelleted by centrifugation (13 000 × rpm, 5 min, 4°C). The supernatant was retained, and protein concentrations were determined using the Plus One 2D Quant kit following the manufacturer's protocol (Amersham Biosciences, Piscataway, NJ). The proteins were stored at −80°C until further use.

2.3 Trypsin digestion and 2-D LC ESI MS/MS

Protein samples (200 μg) were diluted 4 × with 50 mM Tris-Cl (pH 8.0) to reduce the urea concentration prior to trypsin digestion. Proteins were reduced with 5 mM DTT at 65°C for

5 min and alkylated with 10 mM iodoacetamide at 30°C for 30 min. Trypsin digestion used molecular biology grade porcine trypsin (2 μg; 37°C; 16 h; 50:1 ratio of protein/trypsin; Promega, Madison, WI). Tryptic peptides were desalted using a peptide macrotrap (Michrom BioResources, Auburn, CA), eluted in 0.1% TFA 95% ACN solution, vacuum dried, and resuspended in 20 μL of 0.1% formic acid for 2-D LC ESI MS/MS. LC analysis was accomplished by strong cation exchange (SCX) followed by RP LC coupled directly in line with ESI IT mass spectrometer (LCQ Deca XP Plus; ThermoElectron; San Jose, CA) as described [16]. Samples were loaded into an LC gradient ion exchange system containing a Thermo Separations P4000 quaternary gradient pump (ThermoElectron) coupled with a 0.32×100 mm^2 BioBasic SCX column. A flow rate of 3 μL/min was used for both SCX and RP columns. A salt gradient was applied in steps of 0, 10, 15, 20, 25, 30, 35, 40, 45, 50, 57, 64, 90, and 700 mM ammonium acetate in 5% ACN, 0.1% formic acid.

Peptides from SCX were loaded directly into the sample loop of a 0.18×100 mm^2 BioBasic C18 RP LC column of a Proteome X workstation (ThermoElectron). The RP gradient used 0.1% formic acid in ACN and increased the ACN concentration in a linear gradient from 5 to 30% in 30 min and then 30 to 65% in 9 min followed by 95% for 5 min, and 5% for 15 min.

The mass spectrometer was configured to optimize the duty cycle length with the quality of data acquired by alternating between a single full MS scan followed by three MS/MS scans on the three most intense precursor masses (as determined by Xcalibur software in real time) from the full scan. The collision energy was normalized to 35%. Dynamic mass exclusion windows were set at 2 min, and all of the spectra were measured with an overall mass/charge (m/z) ratio range of 300–1700.

2.4 Protein identification

All searches were done using TurboSEQUEST™ (Bioworks Browser 3.2; ThermoElectron) [17]. Mass spectra and tandem mass spectra were searched against an *in silico* trypsin-digested protein database of *S. pneumoniae* TIGR4 downloaded from National Center for Biotechnology Institute (NCBI). Cysteine carboxyamidomethylation and methionine single and double oxidation were included in the search criteria. Peptide identifications were accepted if they exceeded five amino acids long; Xcorr $\geq$1.5, 2.0, and 2.5 for +1, +2, and +3 charged ions, respectively; ΔCn $\geq$0.1. These thresholds were chosen based on decoy searches from a reversed version of the *S. pneumoniae* TIGR4 protein database derived using the reverse database function in Bioworks 3.2. The reversed database was *in silico* trypsin digested and used for searches with tandem mass spectra as described above. The false positive rate for peptide identification at the specified Xcorr/ΔCn thresholds was estimated using a method described for SEQUEST data analysis and was 0.014 [18]. Probabilities of protein identifications being incorrect were calculated using published methods [19, 20] (Supporting Information datasets). Protein identifications were submitted to PRoteomics IDEntification (PRIDE) database [21]: accession numbers 1882 and 1881 (iron replete and restricted, respectively).

2.5 Statistical analysis for protein quantification

We used the computationally intensive "Monte Carlo" statistical method or random resampling with replacement to analyze quantitative changes in protein expression. This approach, unlike parametric methods, makes no *a priori* assumptions about the underlying data distribution and reduces type I errors (false positives). The experimental data were first used to randomly generate (with replacement) replicate *in silico* "experiments". For a protein identified in two groups (*e.g.*, control dataset 1 with A elements and iron restricted dataset 2 with B elements) we used *Protquant*, a variant of spectral counting for relative quantification [22]. When comparing two datasets, *Protquant* utilizes tandem mass spectra present at Xcorr values below the user defined threshold for peptide identification to fill in the missing Xcorr values in a dataset, thus improving the specificity (*i.e.*, decreasing type I errors) provided at least three peptides are identified in the corresponding dataset at user defined identification threshold; the mean difference in the sum of Xcorrs was calculated ($\Delta\Sigma$Xcorr^E) then compared including filled-in missing values that were below the initial Xcorr and ΔCn threshold.

We first generated a "complete profile" of all possible values by pooling the individual Xcorr values for a protein from the two datasets (control and iron restricted) to generate a master list with A + B elements. From the master list, A and B elements were randomly assigned to control and iron restricted groups, and the mean difference in the ΣXcorr was calculated for this synthetic dataset ($\Delta\Sigma$Xcorr^S). Reassignment of experimental data randomly to two groups was repeated 1000 times (*i.e.*, iterations) and the p-value was calculated from the number of the times (M) the $\Delta\Sigma$Xcorr^S was $\geq$ absolute value of $\Delta\Sigma$Xcorr^E (*i.e.*, $p = M/N$). We used a custom software tool for resampling with replacement and p-value calculation. The script for this tool in MATLAB is included as Supporting Information along with example input and output file. The number of replications required for stable estimation of p-value (the convergence) was determined. To correct for multiple testing, we determined the false discovery rate (FDR) for p-value using published methods [23]. Fold-changes in protein expression based on ΣXcorr were estimated as described in ref. [24] and the method accounts for the discontinuity seen in protein identifications where ΣXcorr = 0 in a dataset. We used a correction factor of 0.5 [25] for reporting the $\log_2$ ratio of protein abundance.

2.6 Functional analysis of *S. pneumoniae* TIGR4 proteome

To understand the function of the proteins that we identified from *S. pneumoniae* TIGR4 under iron replete and iron

restricted conditions as differentially expressed, we used Pathway Studio (Ariadne, Rockville, USA) to visualize the TIGR4 proteome in the context of protein interaction networks. The predicted protein interaction network for *S. pneumoniae* was first inferred from the orthologous proteins from Gram-positive bacterial species in the bacterial molecular interaction database of Pathway Studio.

We next identified the Gene Ontology (GO) groups that had significant protein representation in our differentially expressed dataset. Pathway Studio adds further statistical stringency because it calculates the statistical significance of the overlap between the protein list and a GO group using the Fisher exact test (the *p*-value indicates the probability of the overlap occurring by random chance). We used the $p \leq 0.05$ to select GO groups with significant protein representation to build an interaction network that included the upstream regulators and downstream targets of the proteins from the list. In the interaction network, significant changes in protein expression in response to iron restriction were colored dark gray for increased and light gray for decreased expression relative to iron replete growth. Functions of individual proteins with significant changes in expression under iron restricted growth conditions were inferred from UniProt [26].

3 Results and discussion

3.1 *S. pneumoniae* TIGR4 proteome

S. pneumoniae TIGR4 [13] genome has 2105 protein coding regions. We identified 105 and 113 proteins under iron replete and iron restricted growth conditions, respectively (Supporting Information datasets). The intersection between the two datasets was 46 proteins, while 59 and 67 proteins were uniquely identified in iron replete and iron restricted growth conditions, respectively. In our datasets, 50 and 52% of protein identifications were made with single peptides in normal and iron restricted growth conditions, respectively. These numbers are at the lower end of the expected range of proteins identified by single peptide assignments with MudPIT (50–80%) [27] (Supporting Information Table S1).

3.2 Functional analysis: GO groups

We compared the proteome profiles of TIGR4 during growth in iron replete or iron restricted media. We used Pathway Studio and GO functional annotations of *S. pneumoniae* TIGR4 proteins to analyze the genome's functional response to iron restriction. Protein lists from iron replete and iron restricted growth represented 51 and 55 GO groups, respectively. At $p \leq 0.05$, 13 GO groups had significant representation in both datasets and 8 were common to both conditions (Table 1). Each of these GO groups is a unique GO term that corresponds to one of the GO gene product attributes: biological process, molecular function, or cellular component.

GO groups with significant representation under both conditions likely represent fundamental processes necessary for bacterial survival: in our dataset, GO groups with significant representation under both conditions included cytoplasm, cytosolic ribosome, protein biosynthesis, and structural constituents of ribosomes. Polyamine catabolism also appeared to be a fundamental process, as putrescine catabo-

Table 1. Significant GO functional groups represented by *S. pneumoniae* TIGR4 proteome under iron replete and iron restricted growth conditions

Name	GO ID	Dataset[a)]
GTP binding proteins[b)]		1
Nucleobase, nucleoside and nucleotide interconversion	GO:0015949	1
Pentose-phosphate shunt, oxidative branch	GO:0009051	1
Purine ribonucleotide biosynthesis	GO:0009152	1
Pyrimidine nucleotide biosynthesis	GO:0006221	1
Amino acid activation	GO:0006418	2
Fermentation	GO:0006113	2
Gluconeogenesis	GO:0006094	2
Glycolysis	GO:0006096	2
Purine nucleotide biosynthesis	GO:0006164	2
Aminobutyrate catabolism	GO:0009450	3
Cytoplasm	GO:0005737	3
Cytosolic ribosome (sensu bacteria)	GO:0009281	3
Protein biosynthesis	GO:0006412	3
Protein folding	GO:0006457	3
Putrescine catabolism	GO:0009447	3
Structural constituent of ribosome	GO:0003735	3
Translational attenuation	GO:0009386	3

a) 1, Iron replete; 2, iron restriction; 3, both conditions.
b) Pathway studio group.

lism (GO: 0009447) and aminobutyrate catabolism (GO: 0009450) were significantly represented under both conditions. GO groups with significant representation under only one condition (iron replete or iron restricted) revealed differences. Nucleotide metabolism and nucleotide synthesis GO groups were represented in iron replete conditions, while energy metabolism was represented in iron restriction (Table 1).

3.3 Functional analysis: *S. pneumoniae* protein interaction network

Studying the identified proteins in the context of protein interaction networks can help identify the underlying regulatory mechanisms. The bacterial molecular interaction database, built using MedScan™ [28] and available for download in Pathway Studio, does not include *S. pneumoniae* TIGR4. We thus had to first map all 2105 TIGR4 proteins to their corresponding orthologs in the bacterial database by identifying reciprocal-best-BLAST (basic local alignment search tool) hits against *Bacillus subtilis* and *Staphylococcus aureus*. The resulting TIGR4 ortholog map file was imported into Pathway Studio to build an interaction network.

We overlayed our TIGR4 protein data onto the canonical *S. pneumoniae* protein interaction network built in Pathway Studio based on orthologous proteins. The average connectivity of proteins identified in both datasets was 13; *i.e.*, each node (protein) in the network had an average of 13 edges (interactions with other nodes). Protein interaction networks of the 105 and 113 proteins from iron replete and iron restricted growth conditions were built to include all common downstream targets and upstream regulatory proteins (Fig. 1). Some of the upstream and downstream proteins were not identified in this study (*e.g.*, SecA). We did identify the highly connected "party" nodes (which we postulate to be important regulators) chaperonin GroEL (325 edges), cell division protein FtsZ (157 edges), and CTP synthetase (PyrG) (90 edges) (Supporting Information Table S1). However, the protein networks revealed no clear differences between iron replete and iron restricted conditions. Furthermore, a number of proteins in the network have no edges (Fig. 1). Our results show that, though it was possible to carry out network analysis using orthologous proteins and off-the shelf software, a thorough systems analysis of this important "nonmodel" organism requires species specific concerted efforts in both experimental and computational approaches to enable meaningful biological modeling using systems approaches.

3.4 Relative protein quantification

Identification of proteins from biological samples using MS is the first step toward characterizing proteins from a complex sample. However, for capturing precise functional changes in the proteome in response to a stimulus, quantitative differences in protein expression have to be estimated. To accomplish this, label-free and isotopic labeling methods can be used for protein quantification [29]. Several label-free

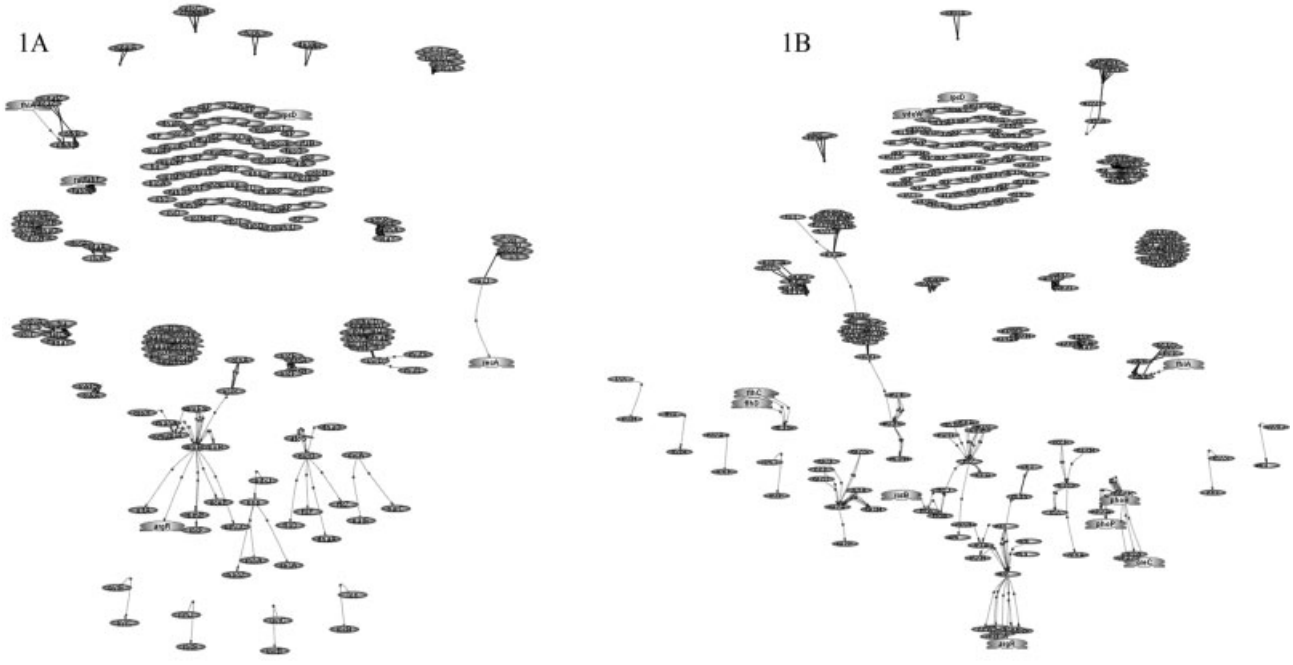

Figure 1. *S. pneumoniae* TIGR4 protein interaction network. *S. pneumoniae* TIGR4 protein interaction network under normal (A) and iron restricted growth conditions (B) visualized in Pathway Studio. Pathways from protein lists were built including common upstream regulators and down stream target proteins.

approaches are available for measuring relative protein abundance, including peptide count [30], spectral count [31], sequence coverage [32], exponentially modified protein abundance index [33], and ΣXcorr which is a refinement of spectral counting that increases the specificity without losing sensitivity [16, 22].

Parametric statistical methods are commonly used for high-throughput proteomic dataset analysis to determine significant changes in protein expression. These methods assume that the differences between the populations under study are normally distributed, but this is a poor assumption for shotgun proteomics [34]. Where this assumption is violated, due to either the biology under investigation or the complexity of sample preparation, processing, and analysis, or even due to small sample sizes common to proteomic studies, it leads to type I errors (*i.e.*, increased false positive significance rate). Nonparametric methods are powerful alternatives for analyzing proteomics data as they do not make any assumptions about the underlying distribution [10]. A common caveat to using nonparametric methods is the loss of statistical power [12]. In contrast, computer-intensive methods offer distribution-free statistics with little or no loss of power and can be adapted to any experimental design. Computer-intensive statistical methods simulate the data thousands of times to generate a sample distribution for the chosen test statistic. Use of computer-intensive methods for proteomic data analysis is relatively new and has been reported with 2-D DIGE [34] and LC MS/MS [35] data.

RR gives a more precise *p*-value estimate than resampling without replacement [11]. RR is especially suitable for analyzing small datasets that have repeated observations like MS/MS data. We applied RR for identifying quantitative differences in TIGR4 proteome expression in response to iron restriction. Convergence was determined for the RR method as a function of number of iterations. We observed that stable estimates of significant changes in protein expression were identified with as little as 50 replications. However, for increased accuracy we did 1000 replications and conducted the analysis ten different times; this provided us a list of 31 proteins that had significantly altered expression in all ten iterations. We used FDR method to correct for multiplicity testing effects and concomitant type I errors [23]. Expression of 31 *S. pneumoniae* proteins changed significantly during growth under iron restricted conditions (Table 2) at FDR adjusted $p \leq 0.05$. While expression of 14 proteins decreased, there was an increase in the expression of 17 proteins under iron restricted growth conditions.

3.5 Significant changes in protein expression: Network analysis

Visualizing proteins with significantly altered expression in response to iron restriction (Table 2) as interaction networks identified PyrG and phosphoenolpyruvate-protein phosphotransferase (PtsI) as nodes with high connectivity (Fig. 2). Expression of PyrG decreased (90 edges; light gray) and PtsI (45 edges; gark gray) expression increased in response to iron restriction. Because there was very little *S. pneumoniae*-specific functional information associated with the edges, we conducted literature searches and used UniProt to decipher the functions of these proteins [26, 36]. PyrG catalyzes the last step in the *de novo* biosynthesis of cytidine triphosphate (CTP) [37] and plays an important role in the synthesis of pyrimidine ribonucleotides. Beyond its function in nucleotide metabolism, PyrG is also a virulence factor in *S. pneumoniae* TIGR4 and a *pyrG*$^{-}$ mutant strain was highly attenuated in mice [38].

PtsI (enzyme I) is the general cytoplasmic component of a carbohydrate active-transport system in bacteria. *S. pneumoniae* TIGR4 can utilize a wide variety of sugars as carbon source, and 30% of the transporters in the genome are predicted to be sugar transporters [13]. Recent studies showed that sucrose transport and metabolism contribute to virulence in murine models of pneumonia [39], which highlights the role of sugars in *S. pneumoniae* metabolism. PtsI mediated phosphorylation of phosphocarrier protein HPr (HPr), a phosphoenolpyruvate dependent "master" regulator of carbon metabolism in Gram positive bacteria leads to HPr-His-P formation. This phosphorylation of HPr by PtsI is required for PTS mediated transport of sugars [40]. PtsI is one of the enzymes that controls the intracellular levels of phosphorylated forms of HPr and directly affects the ratio of Hpr-His-P/Hpr-Ser-P [41], which in turn regulates assimilation of specific carbon (sugar) sources by bacteria. We speculate that alterations in the "general" component of this sugar transport system in response to iron restriction could alter sugar metabolism in *S. pneumoniae* TIGR4 by influencing any of the 21 sugar specific enzyme II complexes.

Overlaying differential protein expression data onto a *S. pneumoniae* protein interaction network helped identify nodes relevant to the biology under investigation (*i.e.*, iron restriction). However, lack of functional information associated with these nodes meant that we had to complement the network analysis with manual literature searches to understand the role of these nodes in normal *S. pneumoniae* physiology as well as virulence. Nevertheless, even this information-scarce network illustrates the power of applying systems approaches to data analysis in identifying biological themes and highlights the need for developing a *S. pneumoniae* protein–protein interaction network.

3.6 Functions of specific proteins with significant changes in expression

The nodes and edges in the protein interaction network of *S. pneumoniae* TIGR4 had very little biological information specific to *S. pneumoniae* pathogenesis, and we could only identify broad descriptive terms for proteins with altered expression. Using *S. pneumoniae* literature and UniProt as described, we found that the functions of differentially expressed proteins encompassed a range of cellular processes including inorganic ion transport, stress response,

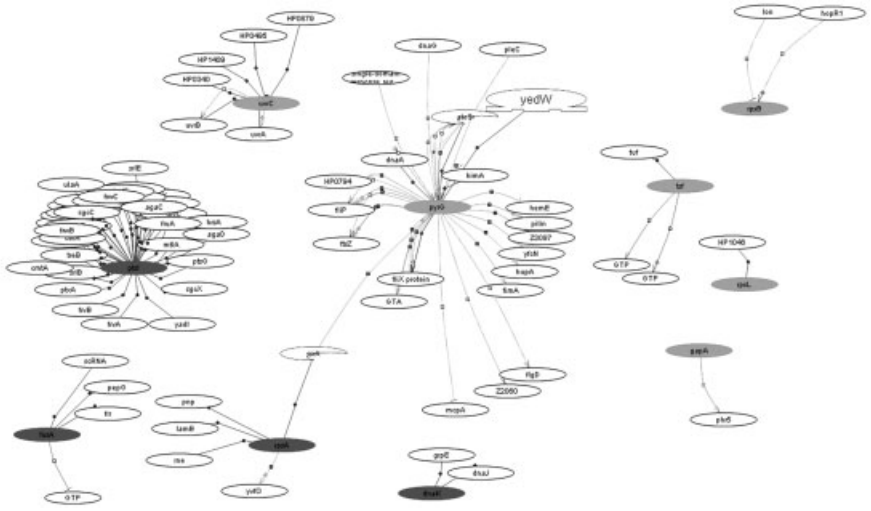

Figure 2. Interaction network of *S. pneumoniae* proteins with significantly altered expression. All 31 proteins from *S. pneumoniae* TIGR4 with significant changes in expression in response to iron restriction were built into an interaction network in Pathway Studio. This network was built including upstream regulators and downstream targets of proteins. A few proteins in the network with high connectivity are shown. Light gray represents decreased expression while dark gray is increased expression and white indicates no significant changes in expression.

DNA synthesis and repair, and translation. The estimated $\log_2$ abundance ratio protein expression change in response to iron restriction was between −4.9- and 4.4-fold (Table 2).

In response to iron restriction, ferritin (an iron binding protein involved in ion transport) expression increased. Ferritin is a DNA protecting protein under starved conditions (DPS) and is induced under metal ion starvation [42]. Ferritin binds to DNA and protects it from oxidative damage from Fe (II) oxidation. Ferritin is also highly immunogenic and is essential for full virulence of *Listeria monocytogenes*, a foodborne Gram-positive human pathogen [26, 43]. Since *S. pneumoniae* growth is not supported by ferritin under iron restriction [44], increased expression of ferritin could constitute a general stress response.

A pneumococcal surface adhesion protein, PsaA, is an attractive candidate for vaccine development as it is highly conserved in all 90 serotypes [45] and immunogenic in all age groups [46]. In mice, immnunization studies with PsaA afforded protection against *S. pneumoniae* carriage [47]. PsaA is involved in the first step of pneumococcal pathogenesis, *i.e.*, colonization of nasopharynx in the host [48]. Increased expression of PsaA in response to iron restriction (Table 2) indicates that *S. pneumoniae* regulates expression of key virulence factors in response to nutrient limitation.

Capsular polysaccharide of *S. pneumoniae* is a major virulence factor and is the basis for classification of up to 90 different serotypes of *S. pneumoniae* [49]. Effects of iron restriction on cell envelope biosynthetic enzymes could have indirect effects on virulence. Our results indicate that expression of uridine diphosphate (UDP)-*N*-acetylglucosamine 2-epimerase decreased four-fold under iron restricted condition, which could result in lowered levels of UDP-*N*-acetyl-D-mannosamine (UDP-ManNac), a capsule precursor [50, 51]. It is likely that reduced concentrations of UDP-ManNAc in response to iron restriction could affect capsule mediated virulence of *S. pneumoniae*; it has been shown that reduced concentrations of another capsule precursor, UDP-glucuronic acid, decreased *S. pneumoniae* type 3 capsule synthesis [52]. We also found increased expression of D-fructose-6-phosphate amidotransferase. A 1.5-fold increase in the expression of this rate-limiting enzyme of the hexosamine biosynthetic pathway can affect intracellular concentrations of the final product of this pathway, UDP-*N*-acetylglucosamine, an essential component of the peptidoglycan of the cell wall and a precursor for many macromolecules [53].

Iron restriction induced *S. pneumoniae* stress response involving altered expression of chaperones. Expression of molecular chaperone DnaK (DnaK) increased 0.8-fold while peptidyl prolyl isomerase (PrsA) expression decreased 2.4-fold. DnaK is crucial for normal folding of native and denatured proteins and prevents the aggregation of proteins under stress conditions: it is critical for cell survival [54], thus even "small" changes in protein expression impact *S. pneumoniae* stress adaptation. DnaK is also is induced by minor changes in temperature [55] and is immunogenic [56]. PrsA, an extracellular protein chaperone, is necessary for secretion of proteins as it plays an important role in post-translocational extracellular protein folding [57, 58]. Furthermore, PrsA is necessary for the production of enzymatically active *Streptococcus* pyrogenic exotoxin B, an important virulence factor in highly invasive group A *Streptococcus* [59]. PrsA is a surface exposed protein in *S. pneumoniae* [13] that elicits antibody response. Mucosal immunization of mice with PsaA and two other surface proteins induces significant protection against pneumococcal pneumonia [60].

Iron restriction affected proteins involved in maintaining DNA structure and integrity. There was a 3.9-fold increase in the expression of UvrC, a protein involved in DNA excision repair. Expression of DNA-binding protein HU, which is associated with the nucleoid and is important for structural organization of the bacterial chromosome, decreased in iron restriction. HU is a DNA architectural protein that bends DNA in a nonsequence specific manner [61]. HU and other

Table 2. List of *S. pneumoniae* TIGR4 proteins with significant changes in expression in response to iron restriction when compared to iron replete growth

Accession	Name	ΣXcorr_Iron replete	ΣXcorr_Iron restriction	Log_2 ratio of abundance[a)]
15901835	Glyceraldehyde-3-phosphate dehydrogenase	25.8	4.5	−2.55
15902018	Elongation factor Ts	22.2	15.4	−0.63
15901337	Elongation factor Tu	32.9	16.3	−1.14
15902019	30S ribosomal protein S2	12.5	5.9	−1.14
15900205	30S ribosomal protein S12	24.6	21	−0.34
15900155	50S ribosomal protein L14	11.3	0	−4.69
15900289	UDP-*N*-acetylglucosamine 2-epimerase	7.7	0	−4.16
15900408	PyrG	8.5	0	−4.29
15900416	Glutamine synthetase, type I	8.1	0	−4.23
15900526	Excinuclease ABC subunit C (UvrC)	6.4	0	−3.90
15900640	Uracil phosphoribosyltransferase	7.1	0	−4.04
15900809	Ribosomal large subunit pseudouridine synthase D	4.9	0	−3.55
15901319	NADH oxidase	12.8	0	−4.87
15901746	Hypothetical protein SP_1922	7.5	0	−4.12
15900200	D-Fructose-6-phosphate amidotransferase	6.4	20.7	1.55
15900858	Peptidylprolyl isomerase (PrsA)	13.4	2.3	−2.44
15900980	DNA-binding protein HU	7.5	27.6	1.75
15900167	Adenylate kinase	2.7	9.7	1.58
15900207	Elongation factor EF-2	3.2	11.4	1.60
15900431	Molecular chaperone DnaK	20.6	37.5	0.78
15900746	30S ribosomal protein S1	5.4	7.1	0.27
15901209	50S ribosomal protein L10	2.2	9.7	1.83
15900145	50S ribosomal protein L3	0	10.5	4.38
15901153	50S ribosomal protein L19	0	6.9	3.80
15901041	PtsI	0	6.5	3.72
15901485	Manganese ABC transporter, manganese-binding adhesion lipoprotein (PsaA)	2.1	7.5	1.53
15901328	Oxidoreductase, aldo/keto reductase family	0	9.4	4.23
15901415	Nonheme iron-containing ferritin	0	6.1	3.63
15901681	Galactokinase	0	9.4	4.23
15901783	DNA-directed RNA polymerase beta' subunit	0	7.5	3.91
15901957	Hypothetical protein SP_2144	0	6.4	3.70

a) Calculated as described in ref. [24].

bacterial histone-like proteins can wrap DNA and stabilize it from denaturation under extreme environmental conditions [26]. Alterations to nucleoid architecture can be linked to changes in global transcription profile and behavior in *E. coli* [62]. Decreased expression of HU with iron restriction could adversely affect all known aspects of HU functionality.

Iron restriction also caused varied effects on expression of *S. pneumoniae* protein synthesis proteins. While expression of ribosomal proteins S1, L3, L10, and L19 increased to a "small" degree, S2, S12, and L14 expression decreased. Ribosomal protein L14 binds 23S rRNA directly. The specific effects of altered ribosomal protein concentrations in *S. pneumoniae* iron restriction response at present are not known; the physiological effects of these changes in protein expression need further evaluation. Expression of translation elongation factors Tu and Ts decreased. Elongation factors mediate binding of aminoacyl tRNA to ribosome site A during protein biosynthesis in a GTP dependent manner. They also catalyze the translocation of nascent polypeptide chain from the A to the P site. Elongation factor Ts is important in *S. pneumoniae* phase variation, which correlates with virulence [63]. *S. pneumoniae* biofilms are involved in tissue infections that encompass pneumonia and meningitis [64] and increased expression of elongation factor EF-2 occurs during *S. pneumoniae* biofilm formation [65]. Iron restriction elicited the same response.

4 Concluding remarks

Pathogenic bacteria have to cope with various host microenvironments for colonization and infection. Understanding the molecular mechanisms of bacterial adaptation to iron restriction can help identify key factors necessary for bacterial growth *in vivo*. However to date, there are no published global analyses of the *S. pneumoniae* response to iron

restriction. Here for the first time, we report quantitative proteomic analysis of *S. pneumoniae*. We showed that under iron limiting growth conditions, *S. pneumoniae* TIGR4 had altered expression of proteins involved in iron transport, manganese transport, sugar metabolism, capsule biosynthesis, and chaperone stress response. Some of the identified proteins, like PsaA, are known virulence factors.

To date, parametric methods have been utilized extensively for determining the statistical significance of protein expression. However, functional genomics technologies like proteomics are inherently expensive which limits the number of biological replicates thus making parametric statistics unappealing. Faced with this limitation, computationally intensive methods to model the distribution of data by random resampling are a logical choice for proteomic data analysis. We applied systems biology paradigms to study *S. pneumoniae* physiology under low-iron conditions at a global proteome level. These methods greatly facilitated our ability to quickly identify key nodes in biological networks, and we speculate that these can potentially be targeted by novel therapeutics. However, while our results demonstrate the utility of studying proteins as interacting entities, our analysis was limited because we had to transfer functions from orthologous proteins (which assumes protein function is conserved) and because of lack of information associated with the edges of the network (which necessitates a thorough manual investigation for functions of all proteins in the network). Therefore, there is a need for implementing available systems biology tools to this pathogen from "model" bacterial species and for developing new computational and experimental tools specific for pneumococcal disease research. Our analysis of the iron restriction response of *S. pneumoniae* TIGR4 proteome constitutes the first step of a systems biology approach for identifying and modeling the regulatory mechanisms that control this bacterial adaptive response.

This project was partially supported by a grant from the National Science Foundation (EPS-0556308-06040293). We acknowledge Dr. Carolyn Boyle, Tibor Pechan, and Allen Shack for technical help. Mass spectrometry analysis was carried out at the Life Sciences and Biosciences Technology Institute, Mississippi State University. This is MAFES publication J11285.

The authors have declared no conflict of interest.

5 References

[1] Eskola, J., Black, S., Shinefield, H., Plotkin, S. A., Orenstein, W. A. (Eds.) in: *Vaccines*, Elsevier, Philadelphia 2004, pp. 589–624

[2] Bridy-Pappas, A. E., Margolis, M. B., Center, K. J., Isaacman, D. J., *Streptococcus pneumoniae:* Description of the pathogen disease epidemiology treatment and prevention. *Pharmacotherapy* 2005, *25*, 1193–1212,

[3] Litwin, C. M., Calderwood, S. B., Role of iron in regulation of virulence genes. *Clin. Microbiol. Rev.* 1993, *6*, 137–149.

[4] Braun, V., Hantke, K., Koster, W., Bacterial iron transport: Mechanisms, genetics, and regulation. *Met. Ions Biol. Syst.* 1998, *35*, 67–145.

[5] Martinez, J. L., Delgado-Iribarren, A., Baquero, F., Mechanisms of iron acquisition and bacterial virulence. *FEMS Microbiol. Rev.* 1990, *6*, 45–56.

[6] Masse, E., Arguin, M., Ironing out the problem: New mechanisms of iron homeostasis. *Trends Biochem. Sci.* 2005, *30*, 462–468.

[7] Nelson, A. L., Barasch, J. M., Bunte, R. M., Weiser, J. N., Bacterial colonization of nasal mucosa induces expression of siderocalin, an iron-sequestering component of innate immunity. *Cell Microbiol.* 2005, *7*, 1404–1417.

[8] Wizemann, T. M., Heinrichs, J. H., Adamou, J. E., Erwin, A. L. *et al.*, Use of a whole genome approach to identify vaccine molecules affording protection against *Streptococcus pneumoniae* infection. *Infect. Immun.* 2001, *69*, 1593–1598.

[9] Mahan, M. J., Slauch, J. M., Mekalanos, J. J., Selection of bacterial virulence genes that are specifically induced in host tissues. *Science* 1993, *259*, 686–688.

[10] Henderson, A. R., The bootstrap: A technique for data-driven statistics. Using computer-intensive analyses to explore experimental data. *Clin. Chim. Acta* 2005, *359*, 1–26.

[11] Pitt, D. G., Kreutzweiser, D. P., Applications of computer-intensive statistical methods to environmental research. *Ecotoxicol. Environ. Saf.* 1998, *39*, 78–97

[12] Potvin, C., Roff, D. A., Distribution-free and robust statistical methods: Viable alternatives to parametric statistics? *Ecology* 1993, *74*, 1617–1628.

[13] Tettelin, H., Nelson, K. E., Paulsen, I. T., Eisen, J. A. *et al.*, Complete genome sequence of a virulent isolate of *Streptococcus pneumoniae*. *Science* 2001, *293*, 498–506.

[14] Tai, S. S., Yu, C., Lee, J. K., A solute binding protein of *Streptococcus pneumoniae* iron transport. *FEMS Microbiol. Lett.* 2003, *220*, 303–308.

[15] Brown, J. S., Gilliland, S. M., Ruiz-Albert, J., Holden, D. W., Characterization of pit, a *Streptococcus pneumoniae* iron uptake ABC transporter. *Infect. Immun.* 2002, *70*, 4389–4398.

[16] Nanduri, B., Lawrence, M. L., Vanguri, S., Burgess, S. C., Proteomic analysis using an unfinished bacterial genome: The effects of subminimum inhibitory concentrations of antibiotics on *Mannheimia haemolytica* virulence factor expression. *Proteomics* 2005, *5*, 4852–4863.

[17] Eng, J. K., McCormack, A. L., Yates, J. R., III, An approach to correlate tandem mass spectral data of peptides with amino acid sequences in a protein database. *J. Am. Soc. Mass Spectrom.* 1994, *5*, 976–989.

[18] Qian, W. J., Liu, T., Monroe, M. E., Strittmatter, E. F. *et al.*, Probability-based evaluation of peptide and protein identifications from tandem mass spectrometry and SEQUEST analysis: The human proteome. *J. Proteome Res.* 2005, *4*, 53–62.

[19] Lopez-Ferrer, D., Martinez-Bartolome, S., Villar, M., Campillos, M. *et al.*, Statistical model for large-scale peptide identification in databases from tandem mass spectra using SEQUEST. *Anal. Chem.* 2004, *76*, 6853–6860.

[20] MacCoss, M. J., Wu, C. C., Yates, J. R., III, Probability-based validation of protein identifications using a modified SEQUEST algorithm. *Anal. Chem.* 2002, *74*, 5593–5599.

[21] Jones, P., Cote, R. G., Martens, L., Quinn, A. F. *et al.*, PRIDE: A public repository of protein and peptide identifications for the proteomics community. *Nucleic Acids Res.* 2006, *34*, D659–D663.

[22] Bridges, S. M., Magee, B. M., Wang, N., Williams, P. W. *et al.*, *ProtQuant*: A tool for the label-free quantification of MudPIT proteomics data. *BMC Bioinformatics* 2007, *8*, S24.

[23] Benjamini, Y.,Hochberg, Y., Controlling the false discovery rate: A practical and powerful approach to multiple testing. *J. R. Stat. Soc. Ser. B* 1995, *57*, 289–300.

[24] Old, W. M., Meyer-Arendt, K., Aveline-Wolf, L., Pierce, K. G. *et al.*, Comparison of label-free methods for quantifying human proteins by shotgun proteomics. *Mol. Cell. Proteomics* 2005, *4*, 1487–1502.

[25] Beissbarth, T., Hyde, L., Smyth, G. K., Job, C. *et al.*, Statistical modeling of sequencing errors in SAGE libraries. *Bioinformatics* 2004, *20*, i31–i39.

[26] UniProt Consortium, The Universal Protein Resource (UniProt). *Nucleic Acids Res.* 2007, *35*, D193–D197.

[27] Kim, J. Y., Lee, J. H., Park, G. W., Cho, K. *et al.*, Utility of electrophoretically derived protein mass estimates as additional constraints in proteome analysis of human serum based on MS/MS analysis. *Proteomics* 2005, *5*, 3376–3385.

[28] Novichkova, S., Egorov, S., Daraselia, N., MedScan, a natural language processing engine for MEDLINE abstracts. *Bioinformatics* 2003, *19*, 1699–1706.

[29] Ong, S. E., Mann, M., Mass spectrometry-based proteomics turns quantitative. *Nat. Chem. Biol.* 2005, *1*, 252–262.

[30] Gao, J., Opiteck, G. J., Friedrichs, M. S., Dongre, A. R., Hefta, S. A., Changes in the protein expression of yeast as a function of carbon source. *J. Proteome Res.* 2003, *2*, 643–649.

[31] Liu, H., Sadygov, R. G., Yates, J. R., III, A model for random sampling and estimation of relative protein abundance in shotgun proteomics. *Anal. Chem.* 2004, *76*, 4193–4201.

[32] Florens, L., Washburn, M. P., Raine, J. D., Anthony, R. M. *et al.*, A proteomic view of the *Plasmodium falciparum* life cycle. *Nature* 2002, *419*, 520–526.

[33] Ishihama, Y., Oda, Y., Tabata, T., Sato, T. *et al.*, Exponentially modified protein abundance index (emPAI) for estimation of absolute protein amount in proteomics by the number of sequenced peptides per protein. *Mol. Cell. Proteomics* 2005, *4*, 1265–1272.

[34] Zhang, B., VerBerkmoes, N. C., Langston, M. A., Uberbacher, E. *et al.*, Detecting differential and correlated protein expression in label-free shotgun proteomics. *J. Proteome Res.* 2006, *5*, 2909–2918.

[35] Chang, J., Van Remmen, H., Ward, W. F., Regnier, F. E. *et al.*, Processing of data generated by 2-dimensional gel electrophoresis for statistical analysis: Missing data, normalization, and statistics. *J. Proteome Res.* 2004, *3*, 1210–1218.

[36] Reid, T., Dunikowski, L. G., PubMed Central–at last. *Can. Fam. Physician* 2006, *52*, 159–160, 165.

[37] Weng, M., Makaroff, C. A., Zalkin, H., Nucleotide sequence of *Escherichia coli* pyrG encoding CTP synthetase. *J. Biol. Chem.* 1986, *261*, 5568–5574.

[38] Hava, D. L., Camilli, A., Large-scale identification of serotype 4 *Streptococcus pneumoniae* virulence factors. *Mol. Microbiol.* 2002, *45*, 1389–1406.

[39] Iyer, R., Camilli, A., Sucrose metabolism contributes to in vivo fitness of *Streptococcus pneumoniae*. *Mol. Microbiol.* 2007, *66*, 1–13.

[40] Titgemeyer, F., Hillen, W., Global control of sugar metabolism: A gram-positive solution. *Antonie Van Leeuwenhoek* 2002, *82*, 59–71.

[41] Deutscher, J., Francke, C., Postma, P. W., How phosphotransferase system-related protein phosphorylation regulates carbohydrate metabolism in bacteria. *Microbiol. Mol. Biol. Rev.* 2006, *70*, 939–1031.

[42] Theil, E. C., Coordinating responses to iron and oxygen stress with DNA and mRNA promoters: The ferritin story. *Biometals* 2007, *20*, 513–521.

[43] Marchler-Bauer, A., Anderson, J. B., Derbyshire, M. K., DeWeese-Scott, C. *et al.*, CDD: A conserved domain database for interactive domain family analysis. *Nucleic Acids Res.* 2007, *35*, D237–D240.

[44] Tai, S. S., Lee, C. J., Winter, R. E., Hemin utilization is related to virulence of *Streptococcus pneumoniae*. *Infect. Immun.* 1993, *61*, 5401–5405.

[45] Morrison, K. E., Lake, D., Crook, J., Carlone, G. M. *et al.*, Confirmation of psaA in all 90 serotypes of *Streptococcus pneumoniae* by PCR and potential of this assay for identification and diagnosis. *J. Clin. Microbiol.* 2000, *38*, 434–437.

[46] Crook, J., Tharpe, J. A., Johnson, S. E., Williams, D. B. *et al.*, Immunoreactivity of five monoclonal antibodies against the 37-kilodalton common cell wall protein (PsaA) of *Streptococcus pneumoniae*. *Clin. Diagn. Lab. Immunol.* 1998, *5*, 205–210.

[47] Briles, D. E., Ades, E., Paton, J. C., Sampson, J. S. *et al.*, Intranasal immunization of mice with a mixture of the pneumococcal proteins PsaA and PspA is highly protective against nasopharyngeal carriage of *Streptococcus pneumoniae*. *Infect. Immun.* 2000, *68*, 796–800.

[48] Romero-Steiner, S., Pilishvili, T., Sampson, J. S., Johnson, S. E. *et al.*, Inhibition of pneumococcal adherence to human nasopharyngeal epithelial cells by anti-PsaA antibodies. *Clin. Diagn. Lab. Immunol.* 2003, *10*, 246–251.

[49] Barocchi, M. A., Censini, S., Rappuoli, R., Vaccines in the era of genomics: The pneumococcal challenge. *Vaccine* 2007, *25*, 2963–2973.

[50] Bentley, S. D., Aanensen, D. M., Mavroidi, A., Saunders, D. *et al.*, Genetic analysis of the capsular biosynthetic locus from all 90 pneumococcal serotypes. *PLoS Genet.* 2006, *2*, e31.

[51] Swartley, J. S., Liu, L. J., Miller, Y. K., Martin, L. E. *et al.*, Characterization of the gene cassette required for biosynthesis of the (alpha1–>6)-linked N-acetyl-D-mannosamine-1-phosphate capsule of serogroup A *Neisseria meningitidis*. *J. Bacteriol.* 1998, *180*, 1533–1539.

[52] Ventura, C. L., Cartee, R. T., Forsee, W. T., Yother, J., Control of capsular polysaccharide chain length by UDP-sugar substrate concentrations in *Streptococcus pneumoniae*. *Mol. Microbiol.* 2006, *61*, 723–733.

[53] Keseler, I. M., Collado-Vides, J., Gama-Castro, S., Ingraham, J. *et al.*, EcoCyc: A comprehensive database resource for *Escherichia coli*. *Nucleic Acids Res.* 2005, *33*, D334–D337.

[54] Gottesman, S., Wickner, S., Maurizi, M. R., Protein quality control: Triage by chaperones and proteases. *Genes Dev.* 1997, *11*, 815–823.

[55] Choi, I. H., Shim, J. H., Kim, S. W., Kim, S. N. *et al.*, Limited stress response in *Streptococcus pneumoniae*. *Microbiol. Immunol.* 1999, *43*, 807–812.

[56] Hamel, J., Martin, D., Brodeur, B. B., Heat shock response of *Streptococcus pneumoniae* Identification of immunoreactive stress proteins. *Microb. Pathog.* 1997, *23*, 11–21.

[57] Kontinen, V. P., Sarvas, M., The PrsA lipoprotein is essential for protein secretion in *Bacillus subtilis* and sets a limit for high-level secretion. *Mol. Microbiol.* 1993, *8*, 727–737.

[58] Jacobs, M., Andersen, J. B., Kontinen, V., Sarvas, M., Bacillus subtilis PrsA is required in vivo as an extracytoplasmic chaperone for secretion of active enzymes synthesized either with or without pro-sequences. *Mol. Microbiol.* 1993, *8*, 957–966.

[59] Ma, Y., Bryant, A. E., Salmi, D. B., Hayes-Schroer, S. M. *et al.*, Identification and characterization of bicistronic speB and prsA gene expression in the group A Streptococcus. *J. Bacteriol.* 2006, *188*, 7626–7634.

[60] Audouy, S. A., van Selm, S., van Roosmalen, M. L., Post, E. *et al.*, Development of lactococcal GEM-based pneumococcal vaccines. *Vaccine* 2007, *25*, 2497–2506.

[61] Sarkar, T., Vitoc, I., Mukerji, I., Hud, N. V., Bacterial protein HU dictates the morphology of DNA condensates produced by crowding agents and polyamines. *Nucleic Acids Res.* 2007, *35*, 951–961.

[62] Kar, S., Edgar, R., Adhya, S., Nucleoid remodeling by an altered HU protein: Reorganization of the transcription program. *Proc. Natl. Acad. Sci. USA* 2005, *102*, 16397–16402.

[63] Overweg, K., Pericone, C. D., Verhoef, G. G., Weiser, J. N. *et al.*, Differential protein expression in phenotypic variants of *Streptococcus pneumoniae Infect. Immun.* 2000, *68*, 4604–4610.

[64] Oggioni, M. R., Trappetti, C., Kadioglu, A., Cassone, M. *et al.*, Switch from planktonic to sessile life: A major event in pneumococcal pathogenesis. *Mol. Microbiol.* 2006, *61*, 1196–1210.

[65] Allegrucci, M., Hu, F. Z., Shen, K., Hayes, J. *et al.*, Phenotypic characterization of *Streptococcus pneumoniae* biofilm development. *J. Bacteriol.* 2006, *188*, 2325–2335.

